Title

Hyperactivated MyD88 signaling in dendritic cells, through specific deletion of Lyn kinase, causes severe autoimmunity and inflammation

Journal

Proceedings of the National Academy of Sciences of the United States of America, 110(35)

ISSN

0027-8424

Authors

Lamagna, Chrystelle
Scapini, Patrizia
van Ziffle, Jessica A
et al.

Publication Date

2013-08-27

DOI

10.1073/pnas.1300617110

Peer reviewed

Hyperactivated MyD88 signaling in dendritic cells, through specific deletion of Lyn kinase, causes severe autoimmunity and inflammation

Chrystelle Lamagna[a], Patrizia Scapini[a,b], Jessica A. van Ziffle[a], Anthony L. DeFranco[c], and Clifford A. Lowell[a,1]

Departments of [a]Laboratory Medicine and [c]Microbiology/Immunology, University of California, San Francisco, CA 94143; and [b]Department of Pathology and Diagnostics, Division of General Pathology, University of Verona, 37134 Verona, Italy

Edited by Michel C. Nussenzweig, The Rockefeller University, New York, NY, and approved July 16, 2013 (received for review January 11, 2013)

Deletion of *lyn*, a Src-family tyrosine kinase expressed by B, myeloid, and dendritic cells (DCs), triggers lupus-like disease in mice, characterized by autoantibody production and renal immune complex deposition leading to chronic glomerulonephritis. B cells from these mice are hyperactive to antigen-receptor stimulation owing to a loss of inhibitory signaling mediated by Lyn kinase. The hyperactive B-cell responses are thought to underlie the development of autoimmunity in this model. Lyn-deficient mice also manifest significant myeloexpansion. To test the contribution of different immune cell types to the lupus-like disease in this model, we generated a *lyn*$^{flox/flox}$ transgenic mouse strain. To our surprise, when we crossed these mice to *Cd11c-cre* animals, generating DC-specific deletion of Lyn, the animals developed spontaneous B- and T-cell activation and subsequent production of autoantibodies and severe nephritis. Remarkably, the DC-specific Lyn-deficient mice also developed severe tissue inflammatory disease, which was not present in the global *lyn*$^{-/-}$ strain. Lyn-deficient DCs were hyperactivated and hyperresponsive to Toll-like receptor agonists and IL-1β. To test whether dysregulation of these signaling pathways in DCs contributed to the inflammatory/autoimmune phenotype, we crossed the *lyn*$^{f/f}$ *Cd11c-cre*$^{+}$ mice to *myd88*$^{f/f}$ animals, generating double-mutant mice lacking both Lyn and the adaptor protein myeloid differentiation factor 88 (MyD88) in DCs, specifically. Deletion of MyD88 in DCs alone completely reversed the inflammatory autoimmunity in the DC-specific Lyn-mutant mice. Thus, we demonstrate that hyperactivation of MyD88-dependent signaling in DCs is sufficient to drive pathogenesis of lupus-like disease, illuminating the fact that dysregulation in innate immune cells alone can lead to autoimmunity.

Lyn tyrosine kinase | conditional dendritic cell mutants | lipopolysaccharide signaling | interleukin 1 signaling

Systemic lupus erythematosus (SLE) is a complex autoimmune inflammatory disease attributed to genetic and environmental factors that cause activation of T and B cells, leading to the formation of autoantibodies and tissue immune complexes. Given that autoantibody production is a hallmark of SLE, most studies have focused on alterations of B-cell tolerance as the main initiator of disease. However, T and myeloid cells are also key players in the pathogenesis of SLE (1, 2). Myeloid expansion is also often observed in SLE, and myeloid-derived cytokines have been found to be major contributors to disease progression in animal models.

Dendritic cells (DCs) are important contributors to the pathogenesis of SLE. However, their precise role is still poorly understood and is complicated by the variety of DC subsets with different functions. The numbers of activated DCs have also been reported to be abnormally high in human SLE patients and mouse models of SLE (3, 4). It is believed that DCs are involved in the development of SLE by promoting autoantibody production by B cells, by their very potent ability to present antigens to T cells, and by producing proinflammatory cytokines and chemokines (5).

The proinflammatory cytokines and chemokines produced by DCs are major contributors to SLE pathogenesis. Exposure to pathogen-associated Toll-like receptor (TLR) ligands triggers the production of proinflammatory cytokines by DCs such as type-1 IFNs, TNF-α, IL-6, IL-12, or IL-1, all of which are critical mediators of autoimmunity. In addition, the capability of DCs to activate naïve T cells depends on their maturation induced by proinflammatory cytokines such as IL-1, TNF-α, or IL-6, or by TLR ligands produced by pathogens (5). Conventional DCs (cDCs) preferentially express TLR2 and TLR4 (and to a lesser extent TLR9 and TLR7), which make them prone to respond to bacterial infections, whereas plasmacytoid DCs (pDCs) are geared to respond to viral infections by preferentially expressing TLR9 and TLR7 (6). Numerous studies using mouse models of SLE or in vitro systems have demonstrated that signaling adapter MyD88-dependent TLR signaling in B cells is involved in the development of autoantibodies (7). However, there have been relatively few studies on the role of TLR signaling in DCs in lupus-like diseases.

Lyn is a Src-family tyrosine kinase (SFK) expressed by B, myeloid, and dendritic cells. Lyn has unique regulatory properties, because it not only triggers activation signals but also mediates inhibitory signals that attenuate cell activation leading to tolerance (1). The role of Lyn in B cells is probably the most extensively described. Lyn functions at the initial step of B-cell receptor (BCR) signaling by phosphorylating tyrosines in the immunoreceptor tyrosine-based activation motifs of BCR-associated proteins, initiating signaling events that lead to cytokine production, proliferation, and migration. Importantly, among the SFK members, Lyn has the sole capability to engage feedback-inhibitory pathways by phosphorylating the immunoreceptor tyrosine-based inhibitory motifs of CD22 and FcγRIIb (8).

Significance

The pathogenesis of systemic lupus erythematosus, a complex autoimmune inflammatory disease triggered by genetic and environmental factors, is generally attributed to defects in lymphocyte function. We show that dendritic cells (DCs) also drive autoimmune disease in mice. Our observations that dysregulation of Toll-like receptor signaling (a key pathway that alerts the immune system of encounter with infectious agents) in DCs alone is sufficient to induce autoimmunity sheds new light on the pathogenesis of this disease. This work implies that DC-specific reduction of Toll-like receptor signaling may prove to be a highly specific approach to reduce the symptoms of autoimmune diseases.

Author contributions: C.L. and C.A.L. designed research; C.L., P.S., and J.A.v.Z. performed research; J.A.v.Z. contributed new reagents/analytic tools; C.L. analyzed data; and C.L., A.L.D., and C.A.L. wrote the paper.

The authors declare no conflict of interest.

This article is a PNAS Direct Submission.

[1]To whom correspondence should be addressed. E-mail: Clifford.Lowell@ucsf.edu.

This article contains supporting information online at www.pnas.org/lookup/suppl/doi:10.1073/pnas.1300617110/-/DCSupplemental.

The role of Lyn in regulation of TLR pathways is somewhat unclear. Initial studies suggested that Lyn is a positive regulator of TLR signaling because it is physically associated with the LPS coreceptor CD14 and becomes activated in LPS-treated monocytes (9). Pharmacologic blockade of Lyn and other SFKs, using rather broad-range inhibitors, leads to a block in TLR4 signaling triggered by LPS (9–11). More recent studies using genetic approaches in mice have proposed that Lyn acts as a positive regulator downstream of TLR4 in mast cells but exerts its negative regulatory function downstream of TLR4 (and TLR2) in macrophages (12, 13).

Mice lacking Lyn represent a well-established model of lupus-like autoimmunity. $Lyn^{-/-}$ mice develop high levels of autoreactive antibodies, leading to severe glomerulonephritis. $Lyn^{-/-}$ B cells have enhanced BCR signaling that leads to impaired tolerance (8, 14). However, $lyn^{-/-}$ mice also have hyperactivated macrophages and DCs, which proliferate over time, causing a dramatic expansion in total myeloid cells, including DCs (1). It remains unclear whether these dysregulated DCs arise as a consequence of the disease or are actually causative to the process.

Recent findings from our laboratory demonstrate that (*i*) in vitro, $lyn^{-/-}$ DCs secrete high levels of cytokines associated with autoimmunity; (*ii*) in vivo, the increase in serum levels of some of these cytokines precedes the generation of autoantibodies; and (*iii*) deletion of Lyn in myeloid cells in $lyn^{-/-}rag\text{-}1^{-/-}$ double-mutant mice causes myeloid expansion, suggesting that the myeloproliferative phenotype observed in $lyn^{-/-}$ mice is only partly dependent on B-cell-mediated autoimmunity (2). Hence, we hypothesized that the autoimmunity in $lyn^{-/-}$ mice is not only due to defects in B cells, but also to the hyperactivation of cells from myeloid and dendritic cell lineages. To directly assess whether dysregulated Lyn-deficient DCs initiate or drive autoimmunity, we generated a $lyn^{flox/flox}$ transgenic mouse ($lyn^{f/f}$), which we crossed with mice carrying the Cre recombinase under the control of the CD11c promoter (*Cd11c-cre*) (15), resulting in deletion of Lyn in DCs. Here we show that the specific deletion of Lyn in DCs was sufficient for the spontaneous activation of B and T cells and the subsequent development of autoantibodies and severe nephritis in mice. Surprisingly, the DC-specific Lyn-deficient mice developed severe inflammation rarely observed in the total $lyn^{-/-}$ animals. Lyn-deficient DCs exhibited a hyperactivated phenotype and were hyperresponsive to TLR agonists and IL-1β stimulation. Interestingly, mice bearing deletion of both Lyn and MyD88 in DCs did not develop inflammation and lupus-like disease. These results demonstrate that hyperactive MyD88-dependent signals develop in $lyn^{-/-}$ DCs and are sufficient to drive pathogenesis of lupus-like disease in mice.

Results

Generation of Mice Lacking Lyn Specifically in DCs. We generated a conditional allele of *lyn* by introducing 34-bp LoxP sites on either side of exons 3 and 4 of the *lyn* gene followed by homologous recombination in embryonic stem cells, which were then used to generate chimeric mice by standard procedures (Fig. S1*A*). The genomic targeting of the *lyn* locus was assessed by Southern blot, and standard screening of gene transmission was assessed by PCR (Fig. S1 *B–D*). The analysis of Lyn protein levels in circulating neutrophils by flow cytometry indicated that expression from the $lyn^{f/f}$ locus was unaltered by insertion of loxP sites (Fig. S1*E*). Mice carrying the $lyn^{f/f}$ locus (back-crossed for nine generations onto the C57BL6 background) were born at expected Mendelian ratios and showed no obvious abnormalities during prenatal and postnatal development.

To investigate the specific role of Lyn in DCs we crossed mice carrying the $lyn^{f/f}$ allele with *Cd11c-cre* transgenic mice (15). The efficiency of deletion of the $lyn^{f/f}$ allele by Cre recombination under the control of the CD11c promoter was determined by intracellular detection of Lyn by flow cytometry using splenocytes from 2-mo-old mice (Fig. S2 shows the efficiency of deletion; Fig. S3 shows the flow cytometry gating strategies used throughout). In the control mice, Lyn was expressed in B, myeloid, cDCs, and pDCs (Fig. S2 *A* and *B*). In agreement with previous reports (15), Lyn expression in the $lyn^{f/f}$ $Cd11c\text{-}cre^{+}$ mice was reduced by 75% and 50% in cDCs and pDCs, respectively. The direct comparison of the mean fluorescence intensity (MFI) of Lyn in cDCs and pDCs showed similar expression levels of Lyn in both DC compartments (Fig. S2*C*). Although low levels of CD11c are expressed by certain myeloid and B-cell populations, we found no significant reduction in Lyn expression in splenic monocytes, macrophages, neutrophils, or B cells in $lyn^{f/f}$ $Cd11c\text{-}cre^{+}$ mice, demonstrating the specificity of Lyn deletion in DCs of $lyn^{f/f}$ $Cd11c\text{-}cre^{+}$ mice. Activated T cells also express low levels of CD11c; however, T cells do not express Lyn.

DC-Specific Lyn Deletion Leads to the Development of Nephritis and Inflammation. Mice were euthanized at 6, 8, and 10 mo of age and their kidneys were analyzed by histology (Fig. 1 and Table S1). As early as 6 mo of age, kidneys from $lyn^{f/f}$ $Cd11c\text{-}cre^{+}$ mice, but not from $lyn^{-/-}$ or controls, showed enlarged glomeruli and increased leukocyte infiltration representative of glomerulonephritis, as well as abundant leukocyte infiltration in the interstitial tissue. By contrast, $lyn^{-/-}$ mice showed signs of glomerulonephritis, without interstitial inflammation, by 8–10 mo of age. In addition, $lyn^{f/f}$ $Cd11c\text{-}cre^{+}$ mice, as well as $lyn^{-/-}$ mice, showed deposition of C3 in the kidney glomeruli (Fig. 1*A* and Table S1) and high levels of autoreactive antibodies in the serum (Fig. 1 *B–E*). Hence, specific deletion of Lyn in DCs alone is sufficient to cause development of immune complex-mediated nephritis in mice.

Mice bearing the selective deletion of Lyn in DCs had an average survival of 8 mo, whereas $lyn^{-/-}$ and control mice lived 14 mo and longer (Fig. 1*F*). Interestingly, $Lyn^{f/f}$ $Cd11c\text{-}cre^{+}$ mice developed visible macroscopic skin lesions starting around 6 mo that usually preceded a decline in health. Histological analyses of different tissues revealed that, by 8 mo, 60–70% of $lyn^{f/f}$ $Cd11c\text{-}cre^{+}$ mice, but none of the $lyn^{-/-}$ or control mice, displayed severe leukocyte infiltration in the lungs, liver, and skin (Fig. 2*A* and Table S1). It is likely that the organ inflammation accounted for the accelerated mortality observed in the $lyn^{f/f}$ $Cd11c\text{-}cre^{+}$ mice.

Cytokines play an important role in the pathogenesis of SLE by stimulating immune-cell activation, leading to organ damage. We measured the concentration of cytokines in the sera of 6-mo-old $lyn^{f/f}$ $Cd11c\text{-}cre^{+}$, $lyn^{-/-}$, and control mice by Luminex bead array (Fig. 2*B*). As previously observed, the $lyn^{-/-}$ mice had elevated levels of Th1 (IFN-γ) and Th17 (IL-17), but not Th2 (IL-4 and IL-13) cytokines, as well as increased levels of IL-6, IL12-p40, G-CSF, GM-CSF and a number of chemokines (KC, MIG, MIP-1α/β and IP10) (16). Similar changes were also observed in the $lyn^{f/f}$ $Cd11c\text{-}cre^{+}$ animals (Fig. 2*B*). However, the DC-specific Lyn-deficient mice showed significantly elevated levels of several inflammatory cytokines/chemokines beyond what was seen in the total $lyn^{-/-}$ mice, including TNF-α, KC, MCP-1, IL-1β, and G-CSF. The dramatic increase in these cytokines/chemokines was likely a major contributor to the exaggerated tissue inflammation in the $lyn^{f/f}$ $Cd11c\text{-}cre^{+}$ mice.

Altogether these data show that the specific deletion of Lyn in DCs is sufficient to initiate an immune-mediated cascade leading to the development of lupus-like disease and tissue inflammation.

Specific Deletion of Lyn in DCs Triggers Severe Splenomegaly and Lymphadenopathy. To evaluate the cellular effects of specific deletion of Lyn in DCs on individual leukocyte populations we analyzed secondary lymphoid organs from 2-, 4-, 6-, 8-, and 10-mo-old mice (Fig. 3*A* and Fig. S4 *A* and *B*). The absence of Lyn in DCs resulted in severe splenomegaly starting at 6 mo of age (Fig. S4*A*). By 10 mo, $lyn^{f/f}$ $Cd11c\text{-}cre^{+}$ mice had spleens 16- and 7.9-fold bigger than those of the control and $lyn^{-/-}$ mice, respectively. In addition, $lyn^{f/f}$ $Cd11c\text{-}cre^{+}$ mice exhibited an increase

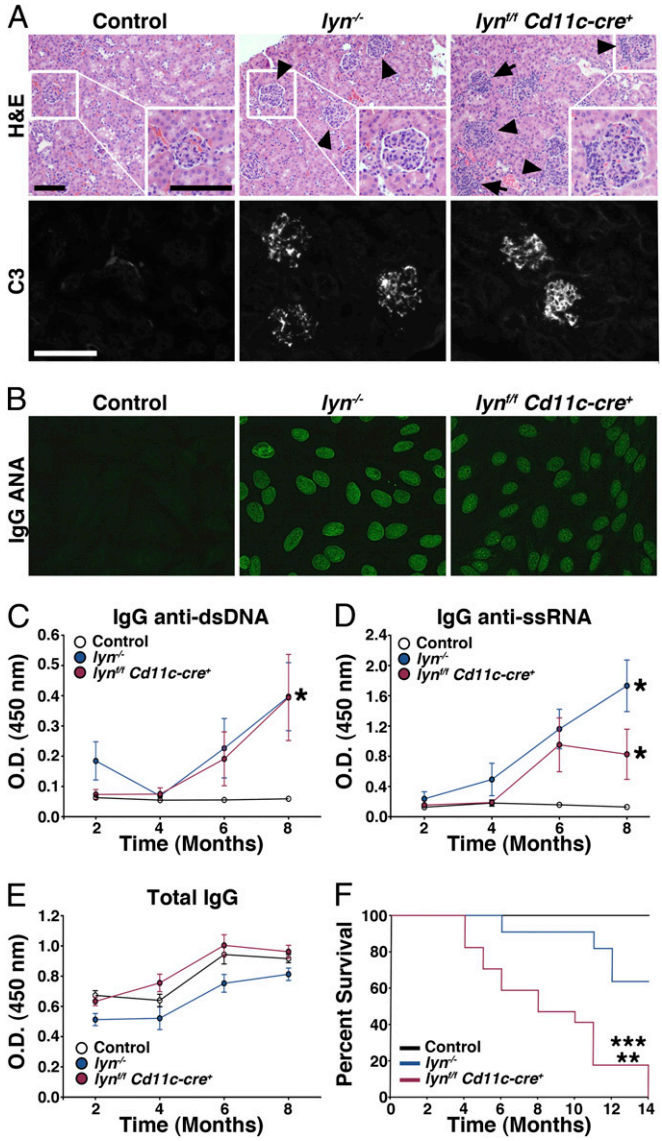

Fig. 1. Specific deletion of Lyn in DCs causes lupus-like autoimmune disease. (*A*) Kidney sections from 8-mo-old control, $lyn^{-/-}$, and $lyn^{f/f}$ *Cd11c-cre*$^{+}$ mice were analyzed for signs of nephritis (H&E staining, *Upper*) and the presence of C3 deposit (*Lower*). Arrowheads and arrows indicate enlarged glomeruli and inflammatory foci, respectively. Representative pictures are shown; the presence and severities of the disease were graded (Table S1). Scale bars, 100 μm. (*B*) Sera from 6-mo-old control, $lyn^{-/-}$, and $lyn^{f/f}$ *Cd11c-cre*$^{+}$ mice were used for detection of IgG ANAs on fixed Hep-2 ANA slides. Representative pictures of six to eight mice per group are shown. (*C*–*E*) Sera from control, $lyn^{-/-}$, and $lyn^{f/f}$ *Cd11c-cre*$^{+}$ mice of the indicated ages were used to monitor the presence of anti-dsDNA (*C*), anti-ssRNA (*D*) autoreactive antibodies, and total Ig (*E*) levels by ELISA. Data represent mean ± SEM from 8–12 mice per group. *$P \leq 0.05$ compared with control (Kruskal–Wallis test). (*F*) Kaplan–Meir analysis of survival of the indicated strains. Each cohort represents 15–20 mice. *$P = 0.0394$ versus control, **$P = 0.0013$ versus $lyn^{-/-}$, ***$P \leq 0.0001$ versus control [log-rank (Mantel–Cox) test].

in lymph node size and cellularity as early as 4 mo of age (Fig. S4*B*). The increased size of the secondary lymphoid organs was mainly due to increased numbers of T cells, myeloid cells, and DCs (Figs. 4*A*, 5*A*, 6*A*, and 7*A*).

B and T Cells Are Spontaneously Activated in Response to the Specific Deletion of Lyn in DCs. It is believed that the development of lupus-like disease in $lyn^{-/-}$ mice is mainly due to the hyperactivated phenotype of their B cells. We analyzed the phenotype of B cells over time in the secondary lymphoid organs of $lyn^{f/f}$ *Cd11c-cre*$^{+}$ mice compared with control and $lyn^{-/-}$ mice. Whereas $lyn^{-/-}$ mice developed B-cell lymphopenia, the $lyn^{f/f}$ *Cd11c-cre*$^{+}$ animals had normal numbers of $CD19^{+}$ B cells in the spleen and lymph nodes, indicating that Lyn deficiency in DCs did not impair B-cell homeostasis (Fig. 3*B* and Figs. S4*C* and S5*A*). Consistent with the presence of autoantibodies in their sera, both $lyn^{f/f}$ *Cd11c-cre*$^{+}$ and $lyn^{-/-}$ animals showed increased numbers of antibody-producing $CD19^{lo/-}$ $CD138^{hi}$ plasma cells in the spleen (Fig. 3*C* and Fig. S4*D*). Whereas the ratio of B cells to plasma cells at 8 mo was 32.2 ± 5.5 in control spleens and 3.9 ± 1.5 in $lyn^{-/-}$ spleens, $lyn^{f/f}$ *Cd11c-cre*$^{+}$ spleens exhibited an intermediate phenotype with a ratio of 10 ± 2. In addition, we found that $lyn^{f/f}$ *Cd11c-cre*$^{+}$ mice exhibited high levels of circulating B-cell activating factor (BAFF), similar to that observed in $lyn^{-/-}$ animals (Fig. 3*D*), suggesting that excessive BAFF production might support survival, activation, and differentiation of plasma cells in $lyn^{f/f}$ *Cd11c-cre*$^{+}$ mice (2). Our results demonstrate that B-cell maturation and isotype switching (to IgG) occurred in $lyn^{f/f}$ *Cd11c-cre*$^{+}$ mice, even though their B cells were not deficient in Lyn, leading to the production of

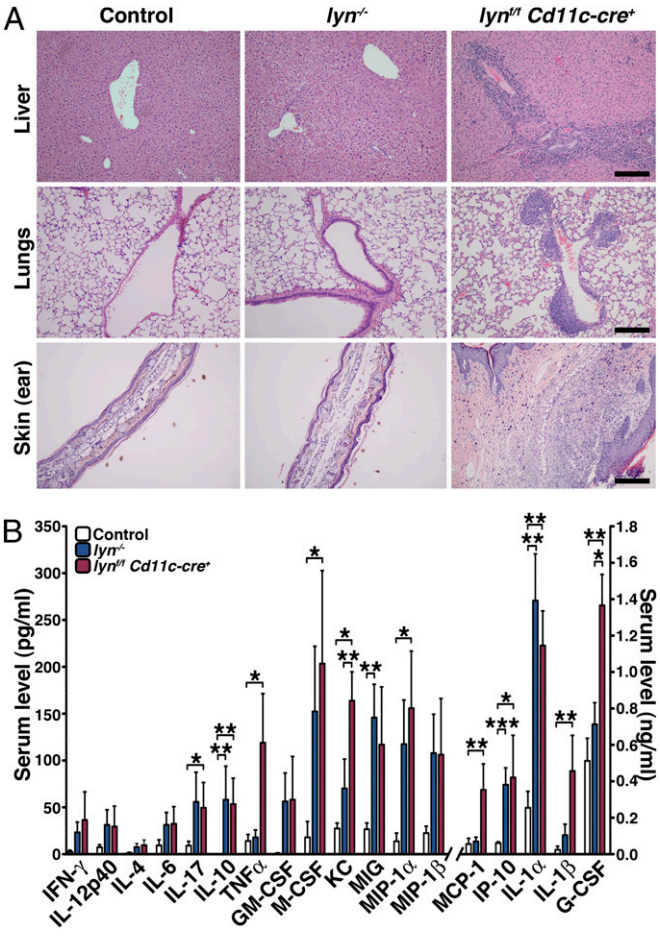

Fig. 2. Specific deletion of Lyn in DCs leads to inflammatory disease in mice. (*A*) Liver, lung, and skin (ear) sections from 8-mo-old control, $lyn^{-/-}$, and $lyn^{f/f}$ *Cd11c-cre*$^{+}$ mice were analyzed (H&E staining) for the presence of inflammatory cell infiltrates. Representative pictures are shown; the presence and severities of leukocyte infiltration were graded (Table S1). Scale bars, 100 μm. (*B*) Cytokine levels from sera of 6-mo-old control ($n = 11$), $lyn^{-/-}$ ($n = 14$), and $lyn^{f/f}$ *Cd11c-cre*$^{+}$ ($n = 14$) mice were determined by Luminex assay. Bars represent mean ± SEM; *$P \leq 0.05$, **$P \leq 0.01$, ***$P \leq 0.001$ (Kruskal–Wallis test).

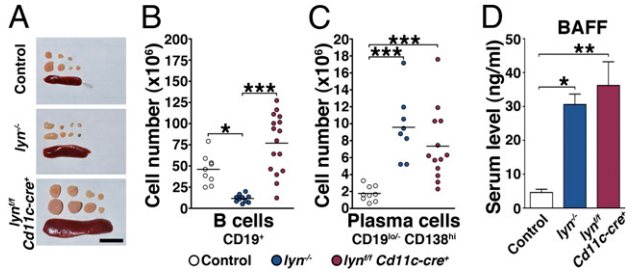

Fig. 3. Lyn in DCs prevents spontaneous activation of B cells in *lyn*$^{f/f}$ *Cd11c-cre*$^{+}$ mice. (*A*) Spleens and cervical lymph nodes were harvested from 8-mo-old control, *lyn*$^{-/-}$, or *lyn*$^{f/f}$ *Cd11c-cre*$^{+}$ mice for analysis. Representative pictures are shown. Scale bar, 1 cm. (*B* and *C*) Absolute numbers of splenic B cells (*B*) and plasma cells (*C*). Data represent mean of independent flow cytometry experiments. Each dot represents an individual mouse. (*D*) BAFF levels in the sera from 6-mo-old control (n = 6), *lyn*$^{-/-}$ (n = 5), and *lyn*$^{f/f}$ *Cd11c-cre*$^{+}$ (n = 9) mice determined by ELISA. Bars represent mean ± SEM; (*B–D*) *$P \le 0.05$, **$P \le 0.01$, ***$P \le 0.001$ (Kruskal–Wallis test).

pathogenic autoantibodies of IgG isotype. Hence, the selective deletion of Lyn in DCs was sufficient to lead to significant activation of B cells in secondary lymphoid organs.

Although T cells do not express Lyn, it has been shown that *lyn*$^{-/-}$ mice have increased numbers of total T cells as well as more activated T cells producing cytokines such as IFN-γ (2). Specific deletion of Lyn in DCs led to a significant increase in the numbers of activated T-cell populations in secondary lymphoid organs (Fig. 4 *A–C* and Figs. S4 *E* and *F* and S5*B*). Surprisingly, the numbers of CD44^{hi} CD62L$^{lo/-}$ effector T cells and CD69^{+} T cells (both CD4^{+} and CD8^{+}) were higher in *lyn*$^{f/f}$ *Cd11c-cre*$^{+}$ than in *lyn*$^{-/-}$ mice. In addition, T cells from *lyn*$^{f/f}$ *Cd11c-cre*$^{+}$ mice were capable of producing IFN-γ, IL-17, and IL-10 in response to LPS stimulation in vivo (Fig. 4*D*). These results suggest that Lyn expression in DCs controlled the homeostasis and activation of the T-cell compartment. To test this hypothesis we adoptively transferred 5-(and -6)-carboxyfluorescein diacetate succinimidyl ester (CFSE)-labeled OT-II CD4^{+} cells into aged control, *lyn*$^{-/-}$, and *lyn*$^{f/f}$ *Cd11c-cre*$^{+}$ mice, followed by immunization with ovalbumin-conjugated anti-DEC205. Three days later, we analyzed the splenic T-cell compartment for OT-II CD4^{+} cell proliferation and activation. *Lyn*$^{f/f}$ *Cd11c-cre*$^{+}$ DCs drove increased T-cell proliferation compared with control and *lyn*$^{-/-}$ DCs and the majority of the transferred OT-II CD4^{+} cells displayed the CD62L$^{lo/-}$ CD44^{hi} effector phenotype and increased CD69 expression level by day 3 following immunization (Fig. 4 *E* and *F*). Interestingly *lyn*$^{-/-}$ mice only showed a moderate increase in proliferation and activation of OT-II CD4^{+} cells compared with

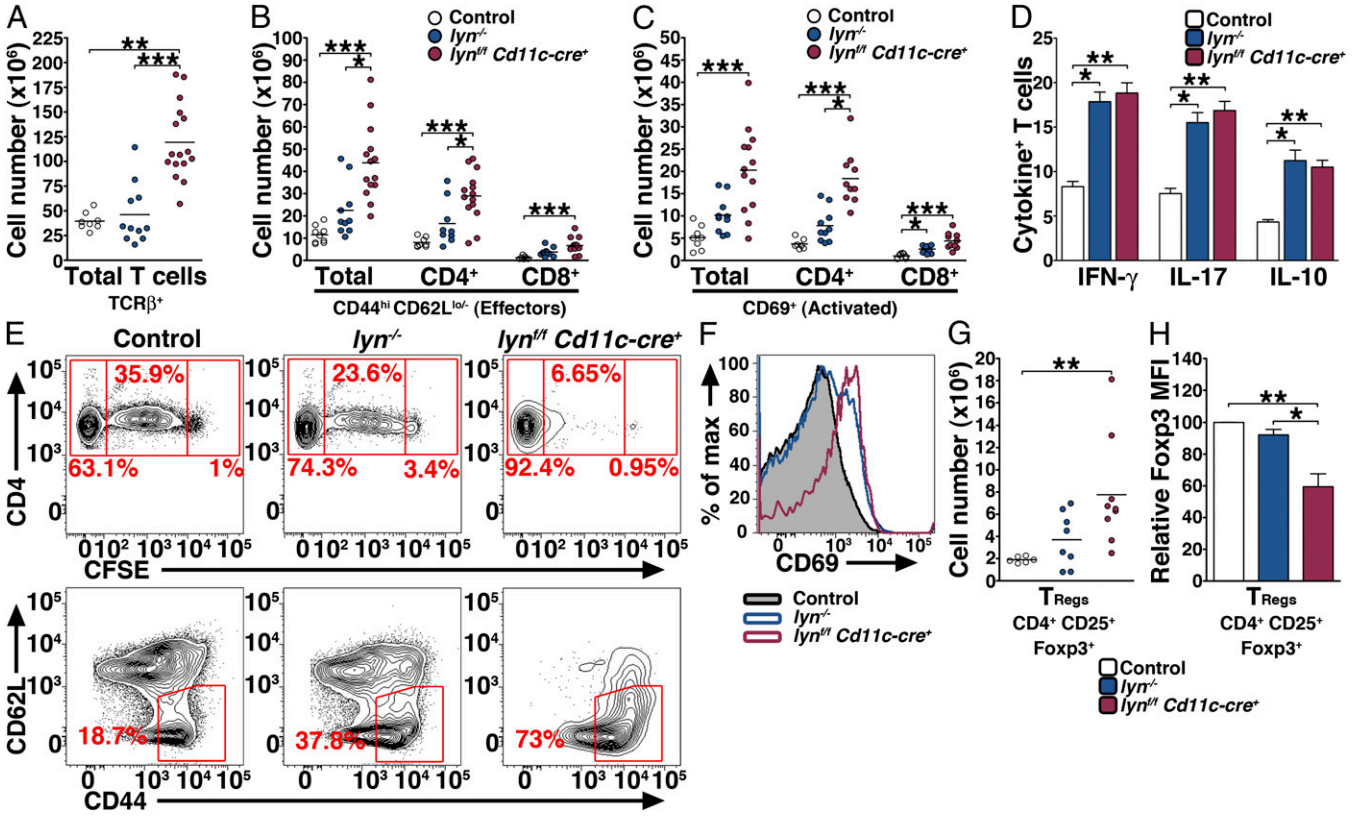

Fig. 4. Lyn-deficient DCs deliver potent signals inducing aberrant proliferation and activation of T cells. Single-cell suspensions were prepared from the spleens and counted, stained, and analyzed by flow cytometry. The absolute numbers of total T cells (*A*), effector T cells (*B*), activated T cells (*C*), and T_{Regs} (*G*) are reported. Data represent mean of independent flow cytometry experiments. Each dot represents an individual mouse. (*D*) Two-month-old control, *lyn*$^{-/-}$, and *lyn*$^{f/f}$ *Cd11c-cre*$^{+}$ mice (n = 8 per group) were coinjected with LPS and Brefeldin A. Four hours later the percentages of splenic T cells producing IFN-γ, IL-17, and IL-10 were determined by intracellular flow cytometry. Bars represent mean ± SEM of independent experiments. (*E* and *F*) Eight-month-old control, *lyn*$^{-/-}$, and *lyn*$^{f/f}$ *Cd11c-cre*$^{+}$ mice (n = 3 per group) were injected 24 h apart with 5 × 10^{6} CFSE-labeled CD4^{+} OT-II cells and 50 μg of ovabulmin-conjugated anti-DEC205 antibody. Three days later single-cell suspensions were prepared from the spleens and the proliferation of OT-II CD4^{+} (*E*, *Upper*), the percentage of transferred OT-II CD4^{+} cells that had converted into effector cells (*E*, *Lower*), and the activation of OT-II CD4^{+} cells (*F*) were analyzed by flow cytometry. Representative FACS profiles are shown. (*H*) Mean fluorescence intensity of Foxp3 (relative to control) expressed by T_{Regs} in 8-mo-old control, *lyn*$^{-/-}$, and *lyn*$^{f/f}$ *Cd11c-cre*$^{+}$ spleens. Bars represent mean ± SEM; (*A–C*, *G*, and *H*) *$P \le 0.05$, **$P \le 0.01$, ***$P \le 0.001$ (Kruskal–Wallis test).

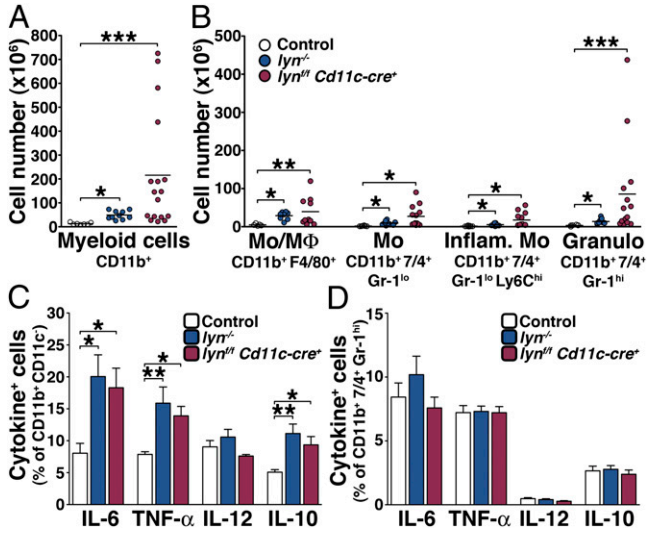

Fig. 5. Myeloid cell phenotypes in the spleens of *lyn*$^{f/f}$ *Cd11c-cre*$^{+}$ mice. (*A* and *B*) Absolute numbers of splenic myeloid cells (*A*) and monocytes/macrophages (Mo/MΦ), monocytes (Mo), inflammatory monocytes (Inflam. Mo.) and granulocytes (*B*) from 8-mo-old control, *lyn*$^{-/-}$, and *lyn*$^{f/f}$ *Cd11c-cre*$^{+}$ mice. Data represent mean of independent flow cytometry experiments. Each dot represents an individual mouse. (*C* and *D*) Two-month-old control, *lyn*$^{-/-}$, and *lyn*$^{f/f}$ *Cd11c-cre*$^{+}$ mice (n = 8 per group) were coinjected with LPS and Brefeldin A. Four hours later the percentages of splenic myeloid CD11b^{+} CD11c^{-} cells (*C*) and granulocytes (*D*) producing IL-6, TNF-α, IL-12, and IL-10 were determined by intracellular flow cytometry. Bars represent mean ± SEM of independent experiments. (*A–D*) $*P \le 0.05$, $**P \le 0.01$, $***P \le 0.001$ (Kruskal–Wallis test).

lyn$^{f/f}$ *Cd11c-cre*$^{+}$ mice. Hence, Lyn-deficient DCs deliver potent signals that induced aberrant proliferation and activation of T cells.

The *lyn*$^{f/f}$ *Cd11c-cre*$^{+}$ mice had elevated numbers of T regulatory (T_{Reg}) cells in the spleens and lymph nodes (Fig. 4*G* and Fig. S5*C*), but the frequency of splenic T_{Regs} within the T-cell compartment was not modified (ratio of T_{Regs}/CD4^{+} effectors: 0.37 ± 0.039 for control mice, 0.36 ± 0.078 for *lyn*$^{-/-}$, and 0.42 ± 0.14 for *lyn*$^{f/f}$ *Cd11c-cre*$^{+}$ mice). By 6 mo of age splenic (but not lymph node) T_{Regs} from the *lyn*$^{f/f}$ *Cd11c-cre*$^{+}$ mice showed significantly lower expression of Forkhead box P3 (Foxp3) compared with control and *lyn*$^{-/-}$ mice (Fig. 4*H* and Fig. S5*D*). However, splenic T_{Regs} from the *lyn*$^{f/f}$ *Cd11c-cre*$^{+}$ mice did not show differences in their capability to produce IL-10 or the proinflammatory cytokines IL-17 and IFN-γ following in vivo stimulation with LPS (Fig. S5*E*). Similarly, no differences in cytokine production (predominately IL-10) were seen in unstimulated T_{Regs} either.

Lyn in DCs Prevents Myeloid Expansion and DC Hyperactivation. Myeloid cell expansion is observed in numerous models of autoimmunity including the *lyn*$^{-/-}$ mice (1). Similarly, *lyn*$^{f/f}$ *Cd11c-cre*$^{+}$ mice displayed a dramatic expansion of the myeloid compartment in the spleen and lymph nodes (Fig. 5 *A* and *B* and Figs. S6 *A–D* and S7 *A–D*). Myeloid cell proliferation occurred earlier in secondary lymphoid organs of *lyn*$^{f/f}$ *Cd11c-cre*$^{+}$ mice compared with *lyn*$^{-/-}$ mice, because the CD11b^{+} populations were already significantly increased at 4 mo in both spleen and lymph nodes (Figs. S6 *A–D* and S7 *A–D*). The numbers of monocytes/macrophages (CD11b^{+} F4/80^{+}), monocytes (CD11b^{+} 7/4^{+} Gr-1^{lo}), which mostly displayed an inflammatory phenotype (CD11b^{+} 7/4^{+} Gr-1^{lo} Ly6C^{hi}), and granulocytes (CD11b^{+} 7/4^{+} Gr-1^{hi}) were all expanded (Fig. 5*B*). The CD11b^{+} CD11c^{-} myeloid cell population from both *lyn*$^{-/-}$ and *lyn*$^{f/f}$ *Cd11c-cre*$^{+}$ mice produced equally high levels of TNF-α, IL-6, and IL-10 following in vivo stimulation with LPS (Fig. 5*C*), despite the fact that CD11b^{+} CD11c^{-} cells in the *lyn*$^{f/f}$ *Cd11c-cre*$^{+}$ mice expressed Lyn

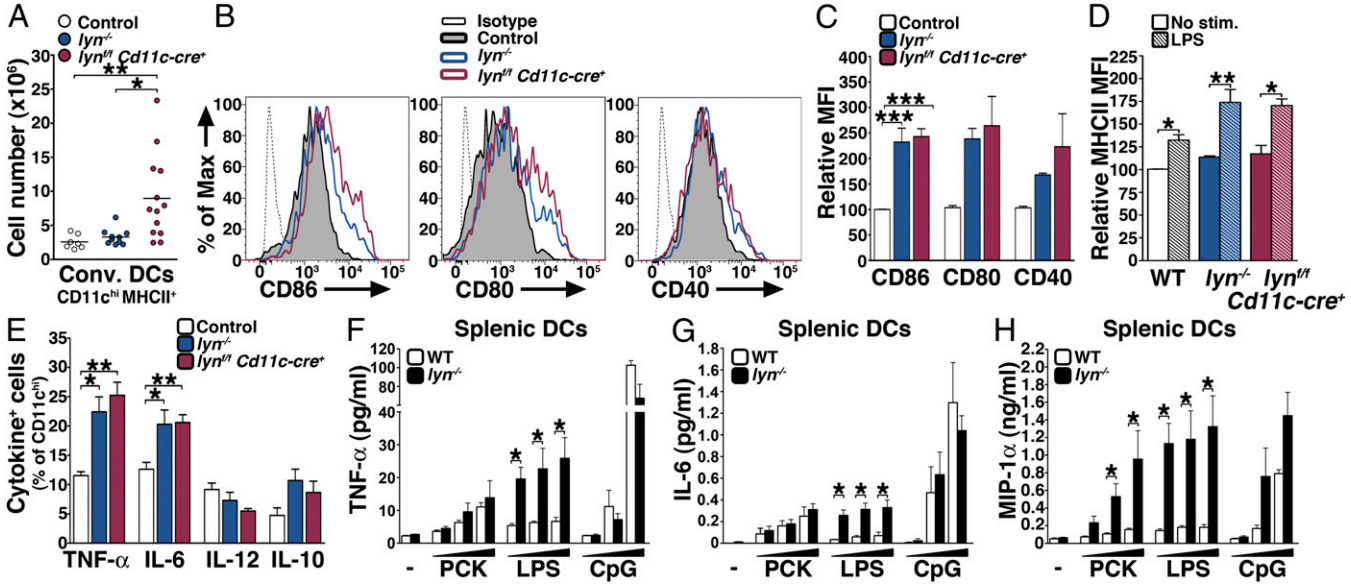

Fig. 6. Lyn-deficient conventional DCs are hyperresponsive to TLR stimulation. (*A*) Absolute numbers of splenic cDCs from 8-mo-old control, *lyn*$^{-/-}$, and *lyn*$^{f/f}$ *Cd11c-cre*$^{+}$ mice. Data represent mean of independent flow cytometry experiments. Each dot represents an individual mouse. (*B*) Representative FACS histogram showing the expression level of CD86, CD80, and CD40 by splenic CD11c^{hi} DCs from 8-mo-old mice. (*C*) MFI (relative to control) of CD86, CD80, and CD40 expressed by CD11c^{hi} DCs in the spleens of 8-mo-old mice. (*D* and *E*) Two-month-old control, *lyn*$^{-/-}$, and *lyn*$^{f/f}$ *Cd11c-cre*$^{+}$ mice (n = 8 per group) were coinjected with LPS and Brefeldin A. Four hours later the relative MFI (relative to unstimulated cells) of MHCII expressed by CD11c^{hi} splenic DCs (*D*) and the percentages of CD11c^{hi} cells producing TNF-α, IL-6, IL-12, and IL-10 (*E*) were determined by flow cytometry. (*F–H*) CD11c^{hi} splenic DCs sorted from 2-mo-old WT and *lyn*$^{-/-}$ mice were stimulated in vitro with 150, 500, or 4,500 ng/mL of Pam3CSK (PCK), LPS, or CpG. Twenty-four hours later the supernatants were collected and the release of TNF-α, IL-6, and MIP-1α were determined by Luminex assay. Bars represent mean ± SEM of three independent experiments. $*P \le 0.05$ (Mann–Whitney test). (*A*, *C–E*) $*P \le 0.05$, $**P \le 0.01$, $***P \le 0.001$ (Kruskal–Wallis test). (*C–E*) Bars represent mean ± SEM of independent experiments from 6–11 mice per group.

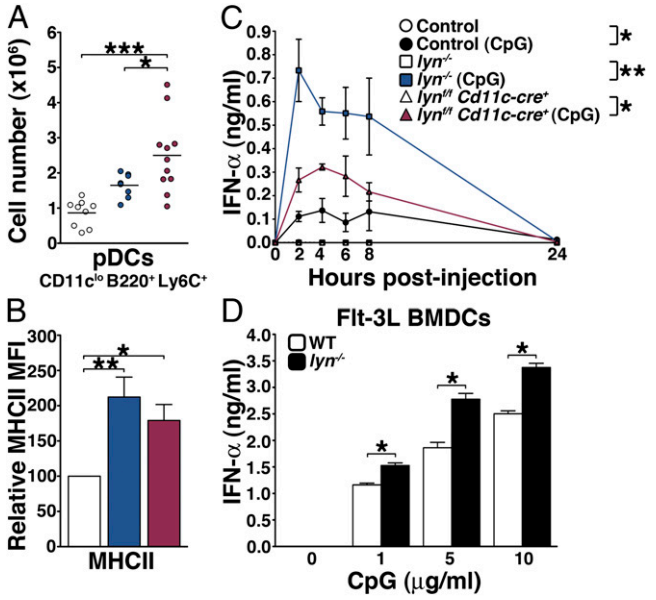

Fig. 7. Lyn-deficient plasmacytoid DCs are hyperresponsive to TLR stimulation. (*A*) Absolute numbers of splenic pDCs from 8-mo-old control, $lyn^{-/-}$, and $lyn^{f/f}$ *Cd11c-cre*$^+$ mice. Data represent mean of independent flow cytometry experiments. Each dot represents an individual mouse. Open circles, control; blue circles, $lyn^{-/-}$; red circles, $lyn^{f/f}$ *Cd11c-cre*$^+$. (*B*) MFI (relative to control) of MHCII expressed by pDCs in the spleens of 8-mo-old mice. (*C*) Two-month-old control, $lyn^{-/-}$, and $lyn^{f/f}$ *Cd11c-cre*$^+$ mice were injected with CpG–DOTAP complexes or DOTAP alone and peripheral blood samples were collected periodically over 24 h. Serum levels of IFN-α were then determined by ELISA. Data represent mean ± SEM from five mice per group and are representative of two independent experiments. $*P \leq 0.05$, $**P \leq 0.01$ (Kruskal–Wallis test). (*D*) BMDCs (generated in the presence of Flt-3L) from WT and $lyn^{-/-}$ mice were stimulated in vitro with 1, 5, or 10 μg/mL of CpG. Twenty-four hours later the supernatants were collected and the release of IFN-α was determined by ELISA. Bars represent mean ± SEM; $*P \leq 0.05$ (Mann–Whitney test).

protein (Fig. S2). Although the numbers of granulocytes were elevated in $lyn^{f/f}$ *Cd11c-cre*$^+$ mice, we did not observe changes in their cytokine production (Fig. 5*D*). Thus, deletion of Lyn in DCs alone is sufficient to induce expansion of the entire myeloid cell compartment. Importantly, Lyn-expressing myeloid cells in $lyn^{f/f}$ *Cd11c-cre*$^+$ mice are hyperresponsive to LPS, suggesting that Lyn-deficient DCs condition Lyn-expressing myeloid cells to become hyperinflammatory.

We next studied the DC populations in secondary lymphoid organs. The numbers of both CD11c^{hi} MHCII$^+$ cDCs and CD11c^{lo} B220$^+$ Ly6C$^+$ pDCs were increased over time in the spleens and lymph nodes of $lyn^{f/f}$ *Cd11c-cre*$^+$ mice, compared with both WT and $lyn^{-/-}$ animals (Figs. 6*A* and 7*A* and Figs. S6 *E* and *F* and S7 *E* and *F*). By 8 mo of age the spleens of $lyn^{f/f}$ *Cd11c-cre*$^+$ mice contained 2.8- and 3.2-fold more cDCs than $lyn^{-/-}$ and control animals, respectively (Fig. 6*A*), and 1.5- and 2.9-fold more pDCs than $lyn^{-/-}$ and control animals, respectively (Fig. 7*A*). Both Lyn-deficient cDCs and pDCs expressed high levels of the costimulatory molecules CD86, CD80, CD40, and MHCII, similar to what was observed in $lyn^{-/-}$ mice, indicative of their activated state (Figs. 6 *B* and *C* and 7*B*).

Production of proinflammatory cytokines in response to infectious agents is an important feature of cDCs. Two-month-old mice were coinjected i.v. with Brefeldin A and LPS and the expression of inflammatory cytokines by cDCs was analyzed by intracellular flow cytometry. After 4 h of in vivo stimulation Lyn-deficient CD11c^{hi} splenic DCs showed increased expression of the activation marker MHCII and produced high levels of inflammatory cytokines such as TNF-α and IL-6 (Fig. 6 *D* and *E*). In addition, Lyn-deficient and WT splenic CD11c^{hi} DCs were sorted from 2-mo-old mice and tested for their propensity to produce cytokines in response to TLR stimulation in vitro (Fig. 6 *F*–*H*). Compared with WT cells, $lyn^{-/-}$ splenic cDCs produced significantly increased amounts of proinflammatory cytokines such as TNF-α and IL-6 in response to TLR4 (LPS), but not TLR2 (Pam3CSK4) or TLR9 (CpG) stimuli. $Lyn^{-/-}$ splenic cDCs also produced increased levels of chemokines such as MIP-1α (Fig. 6*H*). Although splenic cDCs were sorted from young mice (i.e., before the onset of inflammatory disease), one could envision that Lyn-deficient cDCs were conditioned in vivo, as the myeloid cells were, to become hyperinflammatory. To exclude this possibility, we tested the capability of bone marrow-derived DCs generated in the presence of GM-CSF [GM-CSF bone marrow-derived DCs (BMDCs)] to produce proinflammatory cytokines upon exposure to TLR agonists in vitro (Fig. S6 *G*–*I*). Our results showed that $lyn^{-/-}$ GM-CSF BMDCs produced significantly increased amounts of proinflammatory cytokines, to a greater extent than $lyn^{-/-}$ splenic DCs, in response to not only TLR4 but also TLR2 stimuli.

Plasmacytoid DCs are the major source of type-I interferons (IFN-α and -β), which play a central role in SLE pathogenesis (17). We first evaluated the capability of Lyn-deficient pDCs to produce IFN-α over time following in vivo stimulation of TLR9 with CpG–*N*-[1-(2,3-dioleoyloxy)propyl]trimethylammonium methylsulfate (DOTAP) complexes (Fig. 7*C*). Injection of control mice with CpG–DOTAP complexes triggered the elevation of serum IFN-α mediated by pDCs, peaking at 4 h after treatment (Fig. 7*C*). Importantly, IFN-α serum levels in $lyn^{-/-}$ mice injected with CpG–DOTAP complexes were consistently five- to sevenfold higher than those of control mice. In agreement with the observation that pDCs of $lyn^{f/f}$ *Cd11c-cre*$^+$ mice exhibit only 50% reduction of Lyn expression, $lyn^{f/f}$ *Cd11c-cre*$^+$ mice injected with CpG–DOTAP complexes showed a moderate increase in serum levels of IFN-α compared with $lyn^{-/-}$ mice. To demonstrate that pDCs are the source of IFN-α in vivo, we tested the capability of BMDCs generated in the presence of Flt3-L (Flt3-L BMDCs) to produce IFN-α upon exposure to increasing dose of CpG in vitro (Fig. 7*D*). $Lyn^{-/-}$ Flt3-L BMDCs produced significantly increased amounts of IFN-α. Taken together, our results show that both Lyn-deficient cDCs and pDCs are hyperresponsive to TLR stimulation, indicating that Lyn acts as a suppressor of TLR signaling pathways in both cell types.

Lyn Inhibits TLR and IL-1β Signaling in DCs. To elicit the molecular mechanisms leading to hyperactivation of Lyn-deficient DCs and the subsequent development of autoimmune and inflammatory disease in mice, we first tested the capacity of WT or Lyn-deficient GM-CSF BMDCs to activate several signaling pathways such as MAPK, PI3K/Akt, NF-κB and the Jak/Stat pathways (Fig. 8; Fig. S8 *A* and *B* shows quantitation). We found that Lyn itself was activated (as detected by increased phosphorylation at Tyr416 in the activation loop of the kinase domain) upon not only LPS but also IL-1β exposure (Fig. 8*A* and Fig. S8 *A* and *B*). Lyn was phosphorylated within 30 min following LPS stimulation, and within 15 min following IL-1β stimulation. Although Lyn in macrophages exerts its negative function on TLR responses via activation of the PI3K/Akt pathway (12), we did not observe changes in Akt phosphorylation in $lyn^{-/-}$ GM-CSF BMDCs compared with WT upon LPS or IL-1β exposure. By contrast, in the MAPK pathway, Lyn-deficient GM-CSF BMDCs manifested increased Erk activation in response to LPS or IL-1β stimulation, whereas p38 activation remained unchanged (Fig. 8*A* and Fig. S8 *A* and *B*). It is questionable whether BMDCs generated in vitro in the presence of GM-CSF are representative of cDC populations in vivo or of a cell type distinct from the cells that are inactivated in vivo by the *Cd11c-cre* transgene (18). Therefore, we examined

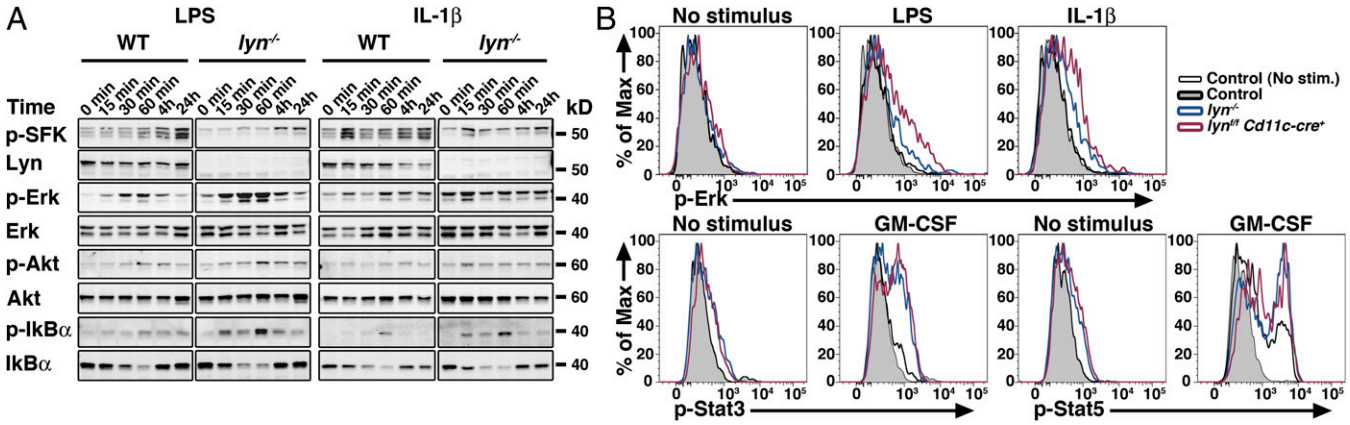

Fig. 8. Lyn signal inhibits MyD88-dependent signals in DCs. (*A*) WT and Lyn-deficient BMDCs (GM-CSF cultures) were exposed to 500 ng/mL LPS or 10 ng/mL IL-1β for the indicated time. Total cell lysates were then subjected to Western-blot analysis to determine the levels of total and phosphorylated (p-) Lyn/SFK (Tyr416), Erk, Akt, and IκBα. Total Erk2 levels were used as loading control. Note that the p-SFK reacts with all Src-family kinases, hence the residual signals in the $lyn^{-/-}$ cells represent Hck and Fgr. Data are representative of three independent experiments. (*B*) Splenocytes from WT, $lyn^{-/-}$, or $lyn^{f/f}$ *Cd11c-cre*$^{+}$ mice were exposed to 500 ng/mL LPS, 10 ng/mL IL-1β, or 50 ng/mL GM-CSF for 20 min. The expression level of p-Erk, p-Stat3, or p-Stat5 in CD11c^{hi} cells was then assessed by phosphoflow cytometry. Representative FACS histograms from two independent experiments are shown.

signaling in splenic cDCs. We observed similar increased Erk activation in splenic CD11c^{hi} DCs isolated from either $lyn^{-/-}$ or $lyn^{f/f}$ *Cd11c-cre*$^{+}$ mice following ex vivo exposure to LPS or IL-1β, as determined by phospho-flow (Fig. 8*B*) or Western blot (Fig. S8 *C* and *D*). In the NF-κB pathway, Lyn-deficient GM-CSF BMDCs or splenic CD11c^{hi} DCs exhibited greater phosphorylation and degradation of IκBα than WT GM-CSF BMDCs in response to LPS or IL-1β exposure (Fig. 8*A* and Fig. S8 *A–D*). However, the increased signaling exhibited by $lyn^{-/-}$ GM-CSF BMDCs was not due to increased levels of TLR4 at the cell surface (Fig. S8 *E* and *F*), indicating that regulation of NF-κB pathways, and not of TLR4 trafficking, is impaired in Lyn-deficient DCs. To determine whether these cells were hyperresponsive to cytokine stimulation, other than IL-1β, we performed phospho-flow cytometry analysis of splenic CD11c^{hi} DCs isolated from either $lyn^{-/-}$ or $lyn^{f/f}$ *Cd11c-cre*$^{+}$ mice exposed to GM-CSF ex vivo. Lyn-deficient DCs showed increased phosphorylation of Stat3 and Stat5 following GM-CSF stimulation (Fig. 8*B*). Hence, we show that Lyn in DCs is activated following stimulation with LPS or IL-1β, and that Lyn-deficient DCs manifest increased Erk and NF-κB pathway activation in response to these stimuli. Because both LPS and IL-1β signal through the adaptor protein MyD88 (19), these results suggest that Lyn may act as a suppressor of MyD88-mediated signaling responses. Our results also indicate that further hyperresponsiveness of Lyn-deficient DCs to cytokines, including GM-CSF and IL-1β, may contribute to the overall disease in both $lyn^{-/-}$ and $lyn^{f/f}$ *Cd11c-cre*$^{+}$ mice.

MyD88 Deletion in Lyn-Deficient DCs Inhibits the Development of Lupus-Like Disease and the Establishment of Proinflammatory Environment. Our results suggest that hyperresponsiveness of Lyn-deficient DCs to MyD88-dependent signals might partly account for subsequent B- and T-cell activation, expansion of the myeloid compartment, and exaggerated inflammation associated with the development of lupus-like disease. To definitively address whether exaggerated MyD88-dependent responses in Lyn-deficient DCs triggers the autoimmune/inflammatory disease in $lyn^{f/f}$ *Cd11c-cre*$^{+}$ mice, we crossed these animals with $myd88^{f/f}$ mice (20) to generate animals whose DCs lack both Lyn and MyD88. Double-mutant $lyn^{f/f}$ $myd88^{f/f}$ *Cd11c-cre*$^{+}$ mice were euthanized at 8 mo of age and their kidneys, lungs, and livers were analyzed for signs of lupus-like disease and organ damage. Kidneys from $lyn^{f/f}$ $myd88^{f/f}$ *CD11c-Cre*$^{+}$ mice were normal in size and cellularity and showed no evidence of leukocyte infiltration, C3 deposition in glomeruli, or interstitial tissue (Fig. 9*A*). In addition, MyD88 deletion in Lyn-deficient DCs reversed the lung and liver inflammation present in single-mutant $lyn^{f/f}$ *Cd11c-cre*$^{+}$ mice. In conjunction with reduced tissue inflammation, the $lyn^{f/f}$ $myd88^{f/f}$ *CD11c-cre*$^{+}$ mice failed to develop autoreactive antinuclear autoantibodies (ANAs), anti-dsDNA, or anti-ssRNA IgG antibodies (Fig. 9*B*). Further analyses of secondary lymphoid organs and their cellular contents showed that MyD88 deletion in DCs was sufficient to reverse the B- and T-cell activation as well as the myeloproliferation present in $lyn^{f/f}$ *Cd11c-cre*$^{+}$ mice. Indeed, the weights of $lyn^{f/f}$ $myd88^{f/f}$ *Cd11c-cre*$^{+}$ spleens and lymph nodes were decreased compared with those in $lyn^{f/f}$ *Cd11c-cre*$^{+}$ mice, reaching the baseline weight observed in control mice (Fig. 9 *C* and *D*). Analysis of splenocytes by flow cytometry revealed that the numbers of B, T, myeloid, and DCs in $lyn^{f/f}$ $myd88^{f/f}$ *Cd11c-cre*$^{+}$ mice were significantly diminished compared with those of $lyn^{f/f}$ *Cd11c-cre*$^{+}$ mice, and similar to those of control mice (Fig. 9 *E–G*). Importantly, deletion of MyD88 in Lyn-deficient DCs completely reversed the hyperactivated phenotype of cDCs and led to the total suppression of B- and T-cell activation observed in $lyn^{f/f}$ *Cd11c-cre*$^{+}$ mice (Fig. 9 *H–K*). Thus, the loss of MyD88-dependent signals in Lyn-deficient DCs completely reversed the autoimmune and inflammatory phenotypes observed in $lyn^{f/f}$ *Cd11c-cre*$^{+}$ mice, providing strong genetic evidence that Lyn acts as a suppressor of MyD88-dependent signaling pathways in DCs in vivo.

Discussion

Although the roles of B and T cells in the development of autoimmunity have been well described, far less is known about the contribution of DCs to autoimmune disease (21). We have generated a $lyn^{f/f}$ conditional knock-out mouse that enables us to assess the role of Lyn in specific cell populations in the pathogenesis of SLE. Here we showed that specific deletion of Lyn in DCs is sufficient for the spontaneous activation of B and T cells, the subsequent development of autoreactive antibodies, and severe nephritis in mice. Surprisingly, mice lacking Lyn in DCs also developed inflammatory disease. Lyn-deficient DCs were hyperactivated and hyperresponsive to bacterial components and cytokines, including GM-CSF and IL-1β. The fact that exaggerated DC responses to TLR and IL-1R activation is driving autoimmunity in $lyn^{f/f}$ *Cd11c-cre*$^{+}$ mice is revealed by the observation that additional deletion of MyD88 in DCs rescues the autoimmune and inflammatory phenotype. Hence, DCs are capable of

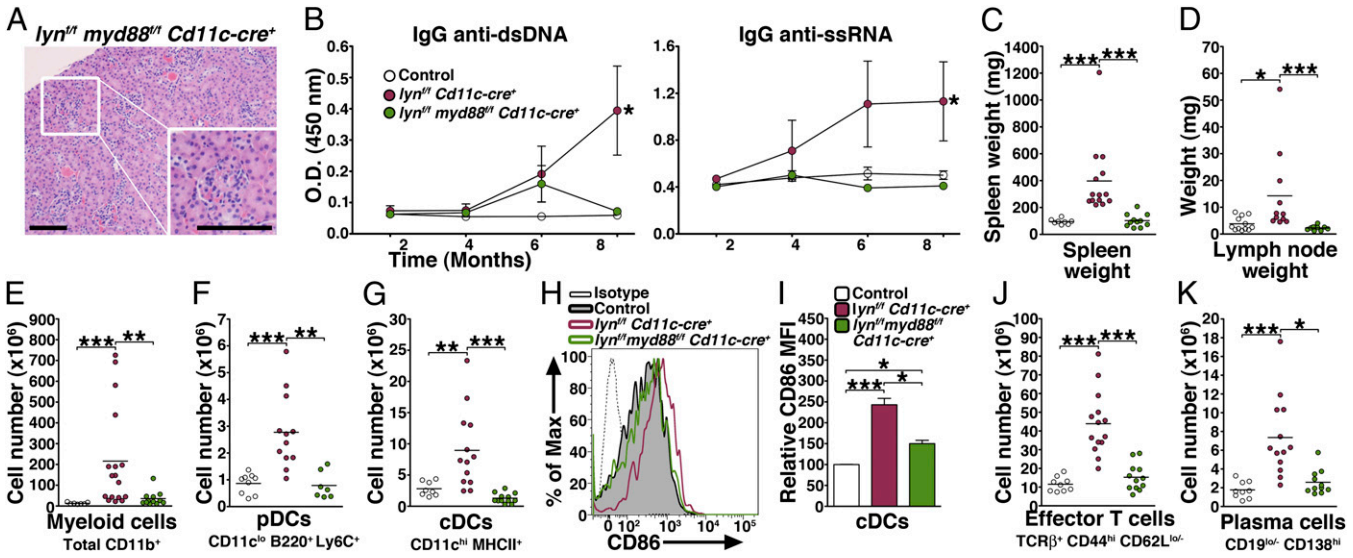

Fig. 9. MyD88 deficiency in DCs rescues the phenotype of *lyn*$^{f/f}$ *Cd11c-cre*$^{+}$ mice. (*A*) *lyn*$^{f/f}$ *myd88*$^{f/f}$ *Cd11c-cre*$^{+}$ mice were euthanized at 8 mo of age and their kidneys were analyzed by histology for signs of nephritis (H&E staining). Representative picture is shown. Scale bars, 100 μm. (*B*) Autoreactive antibodies in the sera from control, *lyn*$^{f/f}$ *Cd11c-cre*$^{+}$, and *lyn*$^{f/f}$ *myd88*$^{f/f}$ *Cd11c-cre*$^{+}$ mice of the indicated ages determined by ELISA. Data represent mean ± SEM from 8–12 mice per group. *$P \leq 0.05$ compared with control and to *lyn*$^{f/f}$ *myd88*$^{f/f}$ *Cd11c-cre*$^{+}$ (Kruskal–Wallis test). (*C* and *D*) Splenic and cervical lymph node weights from 8-mo-old control, *lyn*$^{f/f}$ *Cd11c-cre*$^{+}$, and *lyn*$^{f/f}$ *myd88*$^{f/f}$ *Cd11c-cre*$^{+}$ mice are reported. The absolute numbers of splenic myeloid cells (*E*), plasmacytoid DCs (*F*), conventional DCs (*G*), effector T cells (*J*), and plasma cells (*K*) as determined by flow cytometry are shown. Data represent mean of independent flow cytometry experiments. Each dot represents an individual mouse. Open circles, control; red circles, *lyn*$^{f/f}$ *Cd11c-cre*$^{+}$; green circles, *lyn*$^{f/f}$ *myd88*$^{f/f}$ *Cd11c-cre*$^{+}$. (*H*) FACS histogram showing the expression level of CD86 by CD11c^{hi} splenic DCs from 8-mo-old mice. (*I*) MFI (relative to control) of CD86 expressed by splenic CD11c^{hi} DCs from 8-mo-old mice. Bars represent mean ± SEM of independent experiments from 8–12 mice per group. (*C*–*K*) Data from control and *lyn*$^{f/f}$ *Cd11c-cre*$^{+}$ groups are the same as represented in Figs. 3–7, to perform comparisons to the *lyn*$^{f/f}$ *myd88*$^{f/f}$ *Cd11c-cre*$^{+}$ mice. *$P \leq 0.05$, **$P \leq 0.01$, ***$P \leq 0.001$ (Kruskal–Wallis test).

initiating the autoimmune process. Importantly, we show that MyD88-dependent signals in Lyn-deficient DCs trigger the autoimmune and inflammatory phenotypes observed in *lyn*$^{f/f}$ *Cd11c-cre*$^{+}$ mice. Thus, Lyn in DCs acts as a suppressor of MyD88-dependent inflammatory responses triggered not only by TLRs but also IL-1 signals.

It is surprising that deletion of Lyn in DCs only leads to such an exaggerated inflammatory and autoimmune phenotype compared with *lyn*$^{-/-}$ mice. This suggests that some Lyn-deficient cell type other than DCs, whether hematopoietic or nonhematopoietic, must be partially restraining the inflammatory process in the total *lyn*$^{-/-}$ animals. One can envision that these Lyn-deficient cells prevent the inflammatory disease via the production of anti-inflammatory cytokines in the total *lyn*$^{-/-}$ animals. Indeed, we previously found that Lyn-deficient B cells produce high levels of IL-10 (16). However, we were unable to genetically validate reduced IL-10 production from Lyn-sufficient B cells as the cause of the increased inflammatory disease in DC-specific Lyn-deficient mice, because mice lacking Lyn in both B cells and DCs (generated by crossing *lyn*$^{f/f}$ *Cd11c-cre*$^{+}$ and *Cd79a-cre*$^{+}$ animals) had the same hyperinflammatory phenotype as DC-specific Lyn-deficient mice. Thus, we excluded the possibility that B cells alone in the total *lyn*$^{-/-}$ animals partially restrain the inflammatory process. Interestingly, *lyn*$^{f/f}$ mice crossed with *Vav1-cre*$^{+}$ mice, which induces deletion in all hematopoietic cells, also manifested a hyperinflammatory phenotype, similar to *lyn*$^{f/f}$ *Cd11c-cre*$^{+}$ mice, suggesting that Lyn-mediated signaling in nonhematopoietic cells might have the capacity to counteract the hyperactive Lyn-deficient DCs in *lyn*$^{-/-}$ mice. In addition, although T_{Regs} from *lyn*$^{f/f}$ *Cd11c-cre*$^{+}$ mice exhibit low levels of Foxp3 that have been associated with a reduced suppressive function of these cells (22), we do not observe changes in their capability to secrete proinflammatory cytokines. Nevertheless, it remains a possibility that reduced T_{Reg} function in *lyn*$^{f/f}$ *Cd11c-cre*$^{+}$ mice may contribute to exaggerated inflammatory response in these mice. It is also just as likely that the reduced Foxp3 levels in T_{Regs} in *lyn*$^{f/f}$ *Cd11c-cre*$^{+}$ mice is an effect of the inflammatory state, because Foxp3 levels are reduced in other inflammatory disease models (23). Alternatively, because Lyn-mediated signaling has been linked to apoptosis regulation in neutrophils (24), the loss of Lyn in other immune cell types might limit their lifespan and thus moderate inflammatory disease. Thus, at this point, the cause of the exaggerated inflammatory process in the DC-specific Lyn mutant mouse remains unclear.

What are the cellular consequences of the lack of Lyn regulation of MyD88-dependent signals in DCs? Our study indicates that Lyn-deficient DCs up-regulate T-cell-costimulatory molecules resulting in increased potency to drive T-cell proliferation and activation. Whereas DCs from *lyn*$^{-/-}$ and *lyn*$^{f/f}$ *Cd11c-cre*$^{+}$ animals have a similar degree of up-regulation of costimulatory molecules, *lyn*$^{f/f}$ *Cd11c-cre*$^{+}$ DCs display increased capability to trigger a T-cell response in vivo. This likely results from the fact that *lyn*$^{f/f}$ *Cd11c-cre*$^{+}$ mice have increased numbers of cDCs compared with *lyn*$^{-/-}$ animals, rather than an intrinsic difference between the cDCs themselves. Indeed, the exaggerated expansion of cDCs and pDCs in *lyn*$^{f/f}$ *Cd11c-cre*$^{+}$ mice, leading to excessive T-cell activation, may explain why the DC-specific Lyn-deficient mice have an increased inflammatory phenotype compared with the global *lyn*$^{-/-}$ mutants. Lyn in DCs also prevents MyD88-dependent signals that cause secretion of cytokines such as IL-6, which drive the expansion of the T- and myeloid-cell populations. Finally, a feature of SLE is the impaired clearance and accumulation of autoantigen–autoantibody complexes in tissues that trigger type-I IFN production by pDCs, promoting feedback loops progressively disrupting peripheral immune tolerance and driving disease activity (17). We report a role for Lyn in pDCs in controlling the production of IFN-α in response to TLR9 stimulation.

The role of DCs in autoimmunity is still not fully elucidated and is somewhat controversial. DCs are involved in maintenance of peripheral tolerance and T_{Reg} induction, while also capable of inducing T-cell-mediated autoimmunity (21). The temporary ablation of $CD11c^{hi}$ DCs results in Th1 and Th17 polarization and increased levels of immunoglobulins in the serum of mice, indicating that the absence of DCs is associated with a high risk of autoimmunity (25). However, the constitutive deletion of DCs in CD11c:DTA transgenic mice caused myeloproliferative disorders, but not T-cell-mediated autoimmunity, in one study (26) but was associated to autoimmunity in other studies (27, 28). More recently, the hyperactivation of NF-κB signaling in DCs alone, through DC-specific deletion of the ubiquitin-modifying enzyme A20 using *Cd11c-cre*$^{+}$ mice, led to a dramatic inflammatory/autoimmune syndrome similar to what we observed in *lyn*$^{f/f}$ *Cd11c-cre*$^{+}$ animals in one study and to a striking inflammatory disease but no lupus-like autoimmunity in another study (29, 30). Interestingly, Hammer et al. (29) demonstrated that MyD88-dependent signals in DCs regulate the production of cytokines that drive the expansion of T-cell populations. Our results support the conclusion that hyperactivation of MyD88-mediated signaling pathways in DCs alone can, independently of other genetic changes in other immune cell types, lead to activation of T and B cells, culminating in autoimmune disease.

DCs may contribute to the development of autoimmune diseases through secretion of proinflammatory cytokines. Signals through TLRs on DCs are the major inducers of cytokine release by these cells, and blockade of TLR signaling has been associated with amelioration of autoimmunity. For example, the total knock-out of MyD88 decreases the development of pathogenic autoantibodies and autoimmune nephritis, as well as reducing inflammatory cytokine production, in several mouse models of autoimmunity (31, 32). The use of the relatively new *myd88*$^{f/f}$ mice has allowed us to demonstrate that loss of MyD88 signaling in DCs alone is capable of reversing autoimmunity. It will be important to test the generality of this finding in other autoimmune models. It is important to note that *myd88*$^{-/-}$ mice exhibit a loss in IL-1-mediated signaling as well (19). We found that the rescued phenotype might be related to impaired TLRs and IL-1 functions. Indeed, Lyn-deficient DCs exhibited exaggerated phosphorylation and degradation of IκBα, implying increased NF-κB signaling, following LPS or IL-1β stimulation. We propose that normal commensal flora provide tonic stimulation to the Lyn-deficient DCs to initiate disease development; the hyperactive Lyn-deficient DCs then overproduce inflammatory cytokines, including IL-1α, IL-1β, and GM-CSF, among others, which further primes and activates the Lyn-deficient DCs, leading to even greater responses to endogenous TLR agonists in the fashion of a self-amplifying loop of inflammatory disease. At some point in this self-amplifying loop, T- and B-cell activation occurs, likely in response to cytokines such as IL-12 and BAFF, leading to IFN-γ and autoantibody production, respectively, inducing the full inflammatory and autoimmune phenotype.

Keck et al. (12) reported that Lyn functions as a negative regulator of TLR4 signaling in macrophages, because *lyn*$^{-/-}$ macrophages showed increased activation of the p38 MAPK following LPS stimulation. Our results indicate that Erk, but not p38 MAPK, is activated following MyD88-dependent signals in Lyn-deficient DCs. We also found that Lyn deficiency resulted in dysregulation of NF-κB signaling, similar to what occurs in A20-deficient or SHP-1–deficient DCs (29, 33). Therefore, it is likely that the negative regulatory mechanisms of Lyn on MyD88-dependent pathways in DCs are slightly different from those observed in other myeloid cell types and B cells.

Our observation that dysregulation of MyD88-dependent pathways in DCs alone, through loss of the negative regulatory kinase Lyn, is sufficient to induce autoimmunity sheds light on the pathogenesis of diseases such as SLE. A direct implication of this work is that tyrosine kinase-blocking therapeutics, which currently are being tested in various autoimmune diseases, may have untoward effects on disease progression, mainly through loss of Lyn-mediated inhibitory pathways. In contrast, DC-specific reduction of TLR signaling, which would be expected to have a less dramatic effect on host defense properties than global TLR blockade, may prove to be highly specific for reducing the symptoms of autoimmune diseases.

Methods

Mice. *Lyn*$^{-/-}$, *myd88*$^{f/f}$ and *Cd11c-cre* mice were previously described (1, 15, 20). OT-II mice were kindly provided by Arthur Weiss, University of California, San Francisco (UCSF). Animals were back-crossed at least nine generations onto the C57BL/6 background and kept in a specific pathogen-free facility at UCSF. Animal experiments were done in compliance with the Animal Welfare Act and Regulations, the National Institutes of Health Guide for the Care and Use of Laboratory Animals, the Public Health Service Policy on the Humane Care and Use of Laboratory Animals, and UCSF policies and guidelines. All experiments, except those shown in Figs. 6 *F–H*, 7*D*, and 8*A* and Figs. S6 *G–I* and S8 *A*, *B*, and *E*, were done comparing *lyn*$^{f/f}$ *Cd11c-cre*$^{-}$, *lyn*$^{+/+}$*Cd11c-cre*$^{+}$ and C57BL/6 animals to *lyn*$^{f/f}$ *Cd11c-cre*$^{+}$, *lyn*$^{-/-}$ and *lyn*$^{f/f}$ *myd88*$^{f/f}$ *Cd11c-cre*$^{+}$. The groups *lyn*$^{f/f}$ *Cd11c-cre*$^{-}$, *lyn*$^{+/+}$ *Cd11c-cre*$^{+}$, and C57BL/6 showed similar results. For clarity, the data from these three groups were pooled and defined as the control group.

Flow Cytometry. Single-cell suspensions were prepared from lymphoid organs as previously described (2), blocked with anti-CD16/32 (clone 2.4G2) and murine IgG (Sigma-Aldrich), and stained with the following FITC-, RPE-, APC-, APC-Cy7, or APC-AlexaFluor 780-, PE-Cy7- or biotin-conjugated antibodies from BD PharMingen: CD11c (clone HL3), CD19 (1D3), CD69 (H1.2F3), CD138 (281-2), Gr-1 (RB6-8C5), Ly6C (AL-21), CD40 (3/23), CD80 (16-10A1), MHCII ($I\text{-}A^{b}$, AF6-120.1); from eBiosciences: B220 (RA3-6B2), CD4 (RM4-5), CD8α (53-6.7), CD11b (M1/70), CD25 (PC61.5), CD44 (IM7), CD62L (MEL-14), CD86 (GL1), Foxp3 (FJK-16S), TCRβ (H57-597), TLR4/MD2 (MTS510), and Vα2 TCR (B20.1); from Abcam: 7/4; and from Serotec: F4/80. The rabbit polyclonal antibody anti-mouse Lyn was previously described (2). The gating strategies used to identify the different leukocyte populations by FACS are shown in Fig. S2. For detection of cytokines, mice were coinjected i.v. with 25 μg of LPS from *Escherichia coli*, serotype O111:B4 (Alexis Biochemicals) and 250 μg Brefeldin A (Sigma-Aldrich). Four hours later splenocytes were stained for extracellular markers, fixed, and permeabilized using BD Biosciences reagents according to the manufacturer's instructions, and stained with the following antibodies from eBiosciences: IL-6 (MP5-20F3), IL-10 (JES5-16E3), IL-12 (C17.8), IL-17 (17B7), IFN-γ (XMG1.2), and TNF-α (MP6-XT22). All media contained 10 μg/mL of Brefeldin A. For phosphoflow experiments, splenocytes were stimulated and stained as described in ref. 33 using the following antibodies from BD PharMingen: p-Stat3 (4/P-STAT3) and p-Stat5 (47); or Cell Signaling Technology: p-ERK. Flow cytometry data were collected on a Fortessa flow cytometer (Becton Dickinson) from the UCSF Flow Cytometry Center, and analyzed using FlowJo software (TreeStar). To purify $CD11c^{hi}$ splenic DCs, $CD11c^{+}$ cells were first enriched using Miltenyi Biotec technology. The positive fraction was further sorted on a FACSAria (Becton Dickinson) from the Helen Diller Family Comprehensive Cancer Center Laboratory for Cell Analysis facility at UCSF, to >95% purity.

Histology and ANA Immunofluorescence. Lungs, liver, skin, and kidneys were processed and stained with H&E by the UCSF Pathology core. Kidneys were snap-frozen in optimal cutting temperature compound and 5-μm sections were stained for C3 as previously described (2). For detection of ANA, sera were diluted 1:40 and used for detection of ANAs on fixed Hep-2 ANA slides (Bio-Rad Laboratories) and revealed with FITC-conjugated goat anti-mouse IgG (Jackson ImmunoResearch Laboratories, Inc.). Pictures were acquired using an Eclipse TS100 microscope.

Quantification of Serum IgG, Autoantibodies, and Cytokines. Serum levels of BAFF, total IgG, anti-dsDNA IgG, and anti ss-RNA IgG were determined by ELISA as previously described (2). The levels of IFN-α in the serum or cell culture supernatants were determined by ELISA using VeriKine mouse IFN-α ELISA kit (PBL IFN Source). Cytokine levels in serum or supernatants of splenic DC cultures were quantified using MilliplexMAP mouse cytokine/chemokine kit (Millipore) following the manufacturer's instructions.

Adoptive Transfer and T-Cell Proliferation. For analysis of T-cell proliferation, 5×10^{6} OT-II $CD4^{+}$ cells labeled with 5 μM carboxyfluorescein diacetate

succinimidyl ester (Invitrogen) were adoptively transferred into control, $lyn^{-/-}$, or $lyn^{f/f}$ *Cd11c-cre*$^{+}$ mice. The following day, recipient mice were injected i.v. with 50 μg of ovalbumin-conjugated anti-DEC205 antibody (kindly provided by Audrey Gérard at UCSF). Three days later, single-cell suspensions were prepared from the spleens and the proliferation and activation of OT-II CD4^{+} cells was assessed by flow cytometry.

In Vitro and in Vivo Stimulations with TLR Agonists. Bone marrow-derived DC cultures in the presence of GM-CSF (GM-CSF BMDC) or Flt3-ligand (Flt3-L BMDC) were previously reported (34, 35). Recombinant mouse GM-CSF and Flt3-L were purchased from PeproTech and R&D Systems, respectively. At day 10, the purity of BMDC cultures was assessed by FACS and culture containing at least 85% of CD11c^{+} cells were used for experiments. Sorted splenic DCs or GM-CSF BMDCs (day 10) from 2-mo-old mice were plated at 50,000 cells per well in a 96-well plate in complete medium [RPMI medium 1640 containing 10% heat-inactivated FBS, 2 mM L-glutamine, 2 mM non-essential amino acids, 2 mM sodium pyruvate, 2 mM Hepes (all from UCSF Cell Culture Facility) and 50 μM 2-mercaptoethanol (Sigma-Aldrich)] without GM-CSF and were stimulated with 5, 150, or 4,500 ng/mL of LPS from *E. coli*, serotype O111:B4 (Alexis Biochemicals), Pam3CysSerLys4 (Pam3CSK4; InvivoGen), or HPLC-purified CpG (5′ T*C*C*A*T*G*A*C*G*T*T*C* C*T*G*A*C*G*T*T 3′, where * denotates phosphorothioate bond). Flt3-L BMDCs (day 10) from 2-mo-old mice were plated at 100,000 cells per well in a 96-well plate in complete medium without Flt3-L and exposed to 1, 5, or 10 μg/mL of HPLC-purified CpG. After 24 h the culture supernatants were collected and cytokine levels were assessed.

For in vivo stimulation, 25 μg of HPLC-purified CpG were incubated with 50 μg of DOTAP (Roche), according to manufacturer's instructions, then injected retro-orbitally.

Immunoblotting. GM-CSF BMDCs (day 10, >85% purity), 5×10^{6} per 6-cm dish, were plated in medium containing 0.5% FBS without GM-CSF. Twelve hours later, cells were stimulated with 500 ng/mL LPS (Alexis Biochemicals) or 10 ng/mL IL-1β (PeproTech). Cell lysates were prepared for immunoblotting as described in ref. 33. The following antibodies were used from Cell Signaling Technology: phospho(p)-IκBα Ser32/36, IκBα, p-Akt Ser473, Akt, p-ERK1/2 Thr202/Tyr204, p-SFK (Tyr416); from Santa Cruz Biotechnologies: ERK1/2. Cell surface biotinylation was performed using Sulfo-NHS-LC-Biotin from Pierce, following the manufacturer's instructions. IRDye-conjugated secondary antibodies and infrared Odyssey scanner were used to allow quantitative detection of immunoblotted proteins (LI-COR).

Statistical Analyses. Statistical analyses were performed using GraphPad Prism. The percent survival of $lyn^{f/f}$ *Cd11c-cre*$^{+}$ mice compared with $lyn^{-/-}$ and control mice was determined using the Kaplan–Meir survival analysis [log-rank (Mantel–Cox) test]. Statistical differences between two groups were calculated with a nonparametric Mann–Whitney test. Statistical differences between three groups or more were calculated with a nonparametric Kruskal–Wallis test and a Dunn's multiple comparison posttest.

ACKNOWLEDGMENTS. We thank Clare Abram and Gianna E. Hammer for critical reading of the manuscript, Stanton Glantz for advice on statistical analyses, and Audrey Gérard, Yongmei Hu, Tara Rambaldo, and Mike Lee for help with experiments, animal husbandry, and flow cytometry. This work was supported by National Institutes of Health Grants AI65495 and AI68150 (to C.A.L.) and AI078869 (to A.L.D.), the Basic Research Investment Fund 2012-Futuro in Ricerca (to P.S.), and Ruth L. Kirschstein NRSA Grant 5T32CA009043 (to C.L.).

1. Scapini P, Pereira S, Zhang H, Lowell CA (2009) Multiple roles of Lyn kinase in myeloid cell signaling and function. *Immunol Rev* 228(1):23–40.
2. Scapini P, et al. (2010) Myeloid cells, BAFF, and IFN-γ establish an inflammatory loop that exacerbates autoimmunity in Lyn-deficient mice. *J Exp Med* 207(8):1757–1773.
3. Colonna L, et al. (2006) Abnormal costimulatory phenotype and function of dendritic cells before and after the onset of severe murine lupus. *Arthritis Res Ther* 8(2):R49.
4. Fiore N, et al. (2008) Immature myeloid and plasmacytoid dendritic cells infiltrate renal tubulointerstitium in patients with lupus nephritis. *Mol Immunol* 45(1):259–265.
5. Kis-Toth K, Tsokos GC (2010) Dendritic cell function in lupus: Independent contributors or victims of aberrant immune regulation. *Autoimmunity* 43(2):121–130.
6. Colonna M, Trinchieri G, Liu YJ (2004) Plasmacytoid dendritic cells in immunity. *Nat Immunol* 5(12):1219–1226.
7. Christensen SR, et al. (2005) Toll-like receptor 9 controls anti-DNA autoantibody production in murine lupus. *J Exp Med* 202(2):321–331.
8. Gross AJ, Lyandres JR, Panigrahi AK, Prak ET, DeFranco AL (2009) Developmental acquisition of the Lyn-CD22-SHP-1 inhibitory pathway promotes B cell tolerance. *J Immunol* 182(9):5382–5392.
9. Napolitani G, Bortoletto N, Racioppi L, Lanzavecchia A, D'Oro U (2003) Activation of src-family tyrosine kinases by LPS regulates cytokine production in dendritic cells by controlling AP-1 formation. *Eur J Immunol* 33(10):2832–2841.
10. Orlicek SL, Hanke JH, English BK (1999) The src family-selective tyrosine kinase inhibitor PP1 blocks LPS and IFN-gamma-mediated TNF and iNOS production in murine macrophages. *Shock* 12(5):350–354.
11. Smolinska MJ, Horwood NJ, Page TH, Smallie T, Foxwell BM (2008) Chemical inhibition of Src family kinases affects major LPS-activated pathways in primary human macrophages. *Mol Immunol* 45(4):990–1000.
12. Keck S, Freudenberg M, Huber M (2010) Activation of murine macrophages via TLR2 and TLR4 is negatively regulated by a Lyn/PI3K module and promoted by SHIP1. *J Immunol* 184(10):5809–5818.
13. Avila M, Martinez-Juarez A, Ibarra-Sanchez A, Gonzalez-Espinosa C (2012) Lyn kinase controls TLR4-dependent IKK and MAPK activation modulating the activity of TRAF-6/TAK-1 protein complex in mast cells. *Innate Immun* 18(4):648–660.
14. DeFranco AL, Chan VW, Lowell CA (1998) Positive and negative roles of the tyrosine kinase Lyn in B cell function. *Semin Immunol* 10(4):299–307.
15. Caton ML, Smith-Raska MR, Reizis B (2007) Notch-RBP-J signaling controls the homeostasis of CD8- dendritic cells in the spleen. *J Exp Med* 204(7):1653–1664.
16. Scapini P, et al. (2011) B cell-derived IL-10 suppresses inflammatory disease in Lyn-deficient mice. *Proc Natl Acad Sci USA* 108(41):E823–E832.
17. Obermoser G, Pascual V (2010) The interferon-alpha signature of systemic lupus erythematosus. *Lupus* 19(9):1012–1019.
18. Xu Y, Zhan Y, Lew AM, Naik SH, Kershaw MH (2007) Differential development of murine dendritic cells by GM-CSF versus Flt3 ligand has implications for inflammation and trafficking. *J Immunol* 179(11):7577–7584.
19. Adachi O, et al. (1998) Targeted disruption of the MyD88 gene results in loss of IL-1- and IL-18-mediated function. *Immunity* 9(1):143–150.
20. Hou B, Reizis B, DeFranco AL (2008) Toll-like receptors activate innate and adaptive immunity by using dendritic cell-intrinsic and -extrinsic mechanisms. *Immunity* 29(2):272–282.
21. Platt AM, Randolph GJ (2010) Does deleting dendritic cells delete autoimmunity? *Immunity* 33(6):840–842.
22. Wan YY, Flavell RA (2007) Regulatory T-cell functions are subverted and converted owing to attenuated Foxp3 expression. *Nature* 445(7129):766–770.
23. Murai M, et al. (2009) Interleukin 10 acts on regulatory T cells to maintain expression of the transcription factor Foxp3 and suppressive function in mice with colitis. *Nat Immunol* 10(11):1178–1184.
24. Jia SH, Parodo J, Kapus A, Rotstein OD, Marshall JC (2008) Dynamic regulation of neutrophil survival through tyrosine phosphorylation or dephosphorylation of caspase-8. *J Biol Chem* 283(9):5402–5413.
25. Darrasse-Jèze G, et al. (2009) Feedback control of regulatory T cell homeostasis by dendritic cells in vivo. *J Exp Med* 206(9):1853–1862.
26. Birnberg T, et al. (2008) Lack of conventional dendritic cells is compatible with normal development and T cell homeostasis, but causes myeloid proliferative syndrome. *Immunity* 29(6):986–997.
27. Teichmann LL, et al. (2010) Dendritic cells in lupus are not required for activation of T and B cells but promote their expansion, resulting in tissue damage. *Immunity* 33(6):967–978.
28. Ohnmacht C, et al. (2009) Constitutive ablation of dendritic cells breaks self-tolerance of CD4 T cells and results in spontaneous fatal autoimmunity. *J Exp Med* 206(3):549–559.
29. Hammer GE, et al. (2011) Expression of A20 by dendritic cells preserves immune homeostasis and prevents colitis and spondyloarthritis. *Nat Immunol* 12(12):1184–1193.
30. Kool M, et al. (2011) The ubiquitin-editing protein A20 prevents dendritic cell activation, recognition of apoptotic cells, and systemic autoimmunity. *Immunity* 35(1):82–96.
31. Sadanaga A, et al. (2007) Protection against autoimmune nephritis in MyD88-deficient MRL/lpr mice. *Arthritis Rheum* 56(5):1618–1628.
32. Ehlers M, Fukuyama H, McGaha TL, Aderem A, Ravetch JV (2006) TLR9/MyD88 signaling is required for class switching to pathogenic IgG2a and 2b autoantibodies in SLE. *J Exp Med* 203(3):553–561.
33. Abram CL, Roberge GL, Pao LI, Neel BG, Lowell CA (2013) Distinct roles for neutrophils and dendritic cells in inflammation and autoimmunity in motheaten mice. *Immunity* 38(3):489–501.
34. Gilliet M, et al. (2002) The development of murine plasmacytoid dendritic cell precursors is differentially regulated by FLT3-ligand and granulocyte/macrophage colony-stimulating factor. *J Exp Med* 195(7):953–958.
35. Chu CL, Lowell CA (2005) The Lyn tyrosine kinase differentially regulates dendritic cell generation and maturation. *J Immunol* 175(5):2880–2889.